Available online at www.sciencedirect.com
SCIENCE DIRECT®
Bioorganic & Medicinal Chemistry
Bioorganic & Medicinal Chemistry 13 (2005) 1037–1044

Effects of 8-methyl-2′-deoxyadenosine incorporation into quadruplex forming oligodeoxyribonucleotides

Antonella Virgilio, Veronica Esposito, Antonio Randazzo, Luciano Mayol and Aldo Galeone*

Dipartimento di Chimica delle Sostanze Naturali, Università degli Studi di Napoli 'Federico II', via D. Montesano 49, I-80131 Napoli, Italy

Received 3 August 2004; accepted 19 November 2004
Available online 15 December 2004

Abstract—In this paper we report the synthesis and the structural characterization of two modified oligodeoxyribonucleotides (ODNs), namely d(A^{8Me}GGGT) and d(TA^{8Me}GGGT), where A^{8Me} represents a 8-methyl-2′-deoxyadenosine. Both ODNs have been studied by ^{1}H NMR, CD spectroscopy and molecular modelling and shown to form fourfolds symmetric G-quadruplex structures, with all strands parallel and equivalent to each other. The complexes are characterized by thermal stabilities comparable to that of their natural counterparts. NOE patterns involving 8-methyl group in A^{8Me} residues allowed us to define the main structural features at the 5′-end of the complexes. Particularly, inter- and intrastrand NOEs show a *syn*-orientation and a symmetrical arrangement of A^{8Me} bases stacking on the adjacent G-tetrad.

1. Introduction

G-quadruplex structures are formed in vitro by DNA and RNA oligonucleotides containing runs of guanine bases able to form a variable number of planar arrays of four Gs, named G-tetrads. The interest level in these structures has markedly increased in the past decade as evidence for possible functional roles in vivo have been accumulated. In fact, G-rich sequences occur in several biologically important regions such as chromosomal telomeres, gene promoter regions, recombination sites, RNA packaging sites and RNA dimerization domains.[1–3] Of particular interest is the structural versatility of G-quadruplexes that are able to assume a surprising amount of arrangements differing for the strands stoichiometry and their relative orientation (parallel or antiparallel), as well as the glycosidic angle of guanosine residues (*syn* or *anti*).

A crucial structural feature in G-quadruplex complexes is the relationship between strand orientation and glycosidic conformation of the base moiety: in parallel quadruplexes all G-residues prefer to adopt an *anti*-conformation, while in antiparallel complexes, for each tetrad, two *anti* and two *syn* G-residues are present.[4] However, in a recent publication of some of us[5] the probable occurrence of an all *syn*-tetrad formed by 8-bromo-dG (G^{Br}) residues in the parallel quadruplexes was pointed out. In fact, the presence of a bulky substituent such as the bromine atom at the C8 position, destabilizing the usual *anti*-glycosidic conformation, constrains the residue to adopt a *syn*-orientation of the base. Unexpectedly, one of the resulting tetramolecular quadruplexes, namely [d(TG^{Br}GGT)]$_4$, showed a considerable increase of the thermal stability (about 16 °C) compared to its natural counterpart.

A further contribution to the structural variability of G-quadruplexes comes from the discovery of unusual tetrads such A-tetrads,[6–8] T-tetrads,[9] C-tetrads,[10] mixed tetrads[11] and modified bases containing tetrads[5,12] that increase the number of sequences potentially able to form quadruplexes. Recently, our attention has been addressed to A-tetrads since they are present in several sequences forming tetramolecular parallel quadruplexes (among which the human telomere sequence), where both an all *syn* A-tetrad (AGGGT)[6] and all *anti* A-tetrads (TTAGGGT, TGGAGGC)[7,8] have been found.

Keywords: Quadruplex; 8-Methyl-2′-deoxyadenosine; A-tetrad; Glycosidic conformation.
* Corresponding author. Tel.: +39 081 678542; fax: +39 081 678552; e-mail: galeone@unina.it

0968-0896/$ - see front matter © 2004 Elsevier Ltd. All rights reserved.
doi:10.1016/j.bmc.2004.11.037

In view of the above considerations, we have undertaken the synthesis of 2′-deoxy-8-methyladenosine containing ODNs potentially able to form stable quadruplex structures in order to find a possible connection among relative strand orientation, glycosidic conformation in A-tetrads and thermal stability. In fact, the methyl group at the 8-position, besides promoting the *syn*-glycosidic conformation, should also make easier the structural studies thanks to information possibly arising from NOE contacts, which the methyl proton may establish. Furthermore, 8-methyl-2′-deoxyadenosine could be potentially useful as alternative to 2′-deoxyadenosine in SELEX[13] technology, thus expanding the structural features that could be used for the search of new aptamers.

In this paper, we report the synthesis, CD experiments, NMR and molecular modelling studies of ODNs $A^{8Me}GGGT$ (**I**) and $TA^{8Me}GGGT$ (**II**) (A^{8Me}-ODNs), where A^{8Me} represents 2′-deoxy-8-methyladenosine.

2. Results and discussion

The fundamental step for the synthesis of oligonucleotides containing A^{8Me} is the preparation of the suitably protected A^{8Me} phosphoramidite monomer required for the site-specific incorporation into DNA oligomers. The synthetic strategy of the fully protected A^{8Me} monomer is outlined in Scheme 1.

2′-Deoxyadenosine (**1**) was brominated by treatment with bromine in CH_3COOH/CH_3COONa aqueous buffer according to Eason et al.[14] thus affording 8-bromo-2′-deoxyadenosine (**2**). Compound **2** was protected at 3′ and 5′ hydroxyl functions by HMDS to yield **3** and subsequently transformed into the intermediate **4** following the Van Aershot et al.[15] procedure. Since a partial detachment of protecting groups at 3′ and 5′ functions occurred during the chromatographic purification of **4**, the successive reaction was the well-known transient protection[16] carried out on the partial deprotected intermediates collected from the column. The so obtained N-benzoyl-2′-deoxy-8-methyladenosine (**5**) was treated with 5,5′-dimethoxytritylchloride in dry pyridine[17] for the final protection of the 5′-OH group and the derived compound (**6**) was, in turn, transformed into the corresponding phosphoramidite monomer (**7**) by 2-cyanoethyl-N,N-diisopropyl chlorophosphoramidite.[18] Compound **7** was used for the preparation of the ODNs **I** and **II** following the usual protocols. During the automated syntheses, **7** exhibited similar coupling efficiencies as the common, commercially available, phosphoramidite derivatives.

The ODNs were purified by HPLC, and the fractions containing only full-length products were pooled and used to prepare NMR samples at a concentration of approx 5 mM (0.6 mL, 90% H_2O/10% D_2O), in a 10 mM potassium phosphate, 70 mM KCl, 0.2 mM EDTA (pH 7.0) buffer. ^1H NMR spectra of **I** and **II** were recorded using pulsed-field gradient watergate[19] for H_2O suppression.

The relatively simple appearance of one-dimensional spectra of **I** and **II** indicates that, in the conditions used here, both the modified oligomers mainly form a single well-defined hydrogen-bonded conformation, confidently identified as quadruplexes as described below, having in mind the structures of the unmodified ODNs counterparts. Nevertheless, some weaker resonances attributable to minor forms are present in both the ^1H NMR spectra, whose appearance is not significantly improved by altering the buffer or changing the temperature. Since some of those signals were also present between 11–12 ppm, that is a diagnostic region to identify quadruplex structures, the weaker resonances were attributed to minor quadruplex conformations.

At the temperature of 80 °C, the oligomers result unstructured and only the resonances corresponding to the single strand are present.

As far as 1D proton spectrum of **I** ($T = 30$ °C) is concerned, resonances corresponding to three G-H8 and to T-H6 and A^{8Me}–H2 protons in the aromatic region and two methyl resonances around 1.6 ppm for T-CH_3 and 2.3 ppm for A^{8Me}-CH_3 are observed. Analogously,

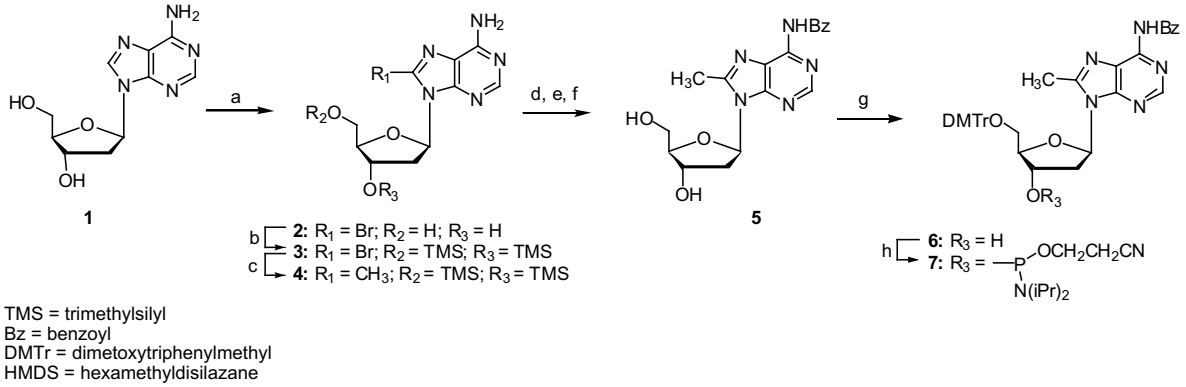

Scheme 1. Synthesis of phosphoramidite derivative **7**. Reagents and conditions: (a) Br_2 in acetate buffer; (b) hexamethyldisilazane, $(NH_4)_2SO_4$ in dry dioxane; (c) $Pd(PPh)_4$, $(CH_3)_4Sn$ in *N*-methylpirrolidinone; (d) trimethylsilyl chloride in dry pyridine; (e) benzoyl chloride in dry pyridine; (f) H_2O/NH_3; (g) dimethoxytriphenylmethyl chloride in dry pyridine; (h) 2-cyanoethyl-N,N-diisopropyl chlorophosphoramidite in dry CH_2Cl_2.

in the case of proton spectrum of **II**, there are only six signals in the aromatic region, whereas, as expected, three methyl resonances are present in the region between 1.5 and 2.5 ppm, where the chemical shift of the methyl group of A^{8Me} is ca. 0.7 ppm further downfield shifted than in thymine. Since resonances from only one strand are observed for both molecules, should the ODNs be structured in multistranded complexes, these must be symmetric.

Furthermore, proton NMR spectra of both **I** and **II** in K^+ containing aqueous solution at a temperature of 30 °C also show three signals in the region 10.5–12 ppm attributable to three exchangeable guanine N1 imino protons. These signals persist at temperature >40 °C and slowly exchange after dilution of the sample into D_2O solution, consistently with the high kinetic stability and low solvent accessibility of quadruplex structures.[20]

Thus, the whole of data suggest that the guanines from each strand form three G-tetrads and the observed number of resonances is consistent with symmetrical four-stranded quadruplexes with all strands equivalent to each other.

The proton decoupled phosphorus spectra of both **I** and **II** in D_2O at 30 °C show that all ^{31}P signals are clustered within −0.8 and −2.2 ppm region, characteristic of unperturbed backbone phosphates of parallel stranded quadruplexes.[21–23]

Moreover, circular dichroism (CD) data (Fig. 1), acquired for both samples at 30 °C, further inferred the formation of parallel quadruplexes. In fact, the presence of a maximum and minimum Cotton effects at 262–264 nm and 243 nm, respectively, are typical of quadruplex involving four parallel strands.[24]

In spite of the little structural heterogeneity observed for both complexes, we were able to perform both resonance assignments (Table 1) and structural studies of the main species present in solution. Particularly, NOESY and TOCSY spectra, obtained at 500 MHz ($T = 30$ °C) for both molecules (see experimental section), showed well dispersed cross peaks, so both exchangeable and nonexchangeable protons could be nearly completely assigned following the standard procedures.[25] The observed NOEs among G-H8/T-H6 and their own H1′, H2′ and H2″ sugar protons and the H1′, H2′ and H2″ protons of the preceding residue (Fig. 2) suggested that both quadruplexes adopt a right handed helical winding. Moreover, PE-COSY spectra analysis indicates that H1′/H2′ coupling constants are reasonably large, thus suggesting that the sugar geometries are predominantly S-type. Therefore, the structure of each strand may be taken to be similar to B-DNA form.

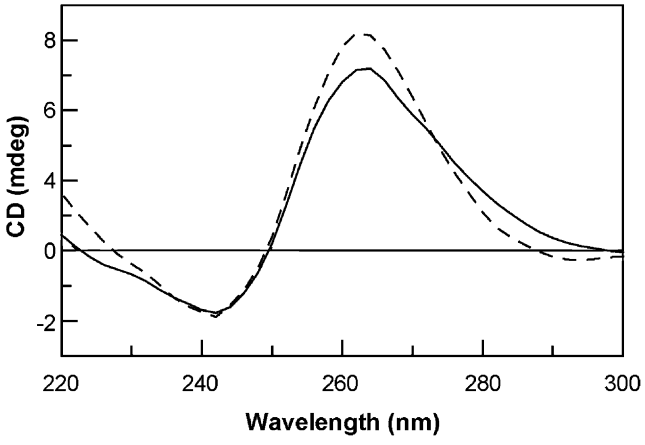

Figure 1. CD spectra of **I** (——) and **II** (---).

As for the glycosidic torsion angles, useful information could be obtained comparing the relative intensities of NOEs between H8/H6 and H2′ and H8/H6 and H1′ protons of the same residue. All Gs and Ts resulted to possess an *anti*-glycosidic conformation, while the modified adenosines (A^{8Me}) adopt a *syn*-conformation, showing intense NOEs between methyl group in 8-position and H1′ sugar proton and more weak crosspeaks between methyl and H2′.

It is interesting to note that the normal sequential connectivities path is broken at 5′-T A^{8Me}-3′ step since the *syn*-orientation of the modified base places the protons of methyl group in 8-position to a distance greater than 6 Å away from the sugar protons on the neighboring 5′ nucleotide.[26]

Furthermore, NMR data of both **I** and **II** show a number of NOE connectivities involving A^{8Me} bases. Particularly, the presence of interstrand NOEs between the methyl group of an A^{8Me} residue and the H2 proton of the modified base on the adjacent strand (Fig. 2), and intrastrand NOEs between A^{8Me} protons nucleotides and the protons of the adjacent Gs on the same strand suggest that A^{8Me} residues are not randomly oriented and are in mutual close proximity arranging in a symmetrical fashion and stacking on the top of G-tetrads in both $[d(A^{8Me}GGGT)]_4$ and $[d(TA^{8Me}GGGT)]_4$. Unfortunately, no clearly resolved resonances for the 6-NH_2 group (indicating the formation of H-bonds) of A^{8Me} bases could be observed.

Crosspeaks in the NOESY spectra (D_2O, mixing time = 180 ms) of quadruplexes **I** and **II** are reasonably well dispersed, allowing the quantization of the experimental NMR data. The distance restraints, deduced from the Overhauser effect intensities by the tool CALIBA of the program CYANA,[27] were used at the various stages of the calculations (see experimental section) to determine the three-dimensional structure of the complexes formed by **I** and **II**. Hydrogen-bond distance restraints about three layers of G-tetrad were also incorporated during the computations. Particularly, 336 distance constraints for **I** and 320 for **II** were derived from NOE peak intensities and reduced to 206 and 160, respectively, after removal of the irrelevant ones, and 24 H-bonds (48 distance restraints: HN1–O6, N1–O6, HN2–N7, N2–N7) were took into account during the

Table 1. Nonexchangeable and imino protons chemical shifts (500 MHz) for [d(A^{8Me}GGGT)]$_4$ and [d(TA^{8Me}GGGT)]$_4$ quadruplexes in 10 mM KH_2PO_4, 70 mM KCl, 0.2 mM EDTA (pH 7.0, T = 30 °C)

Base (5′–3′)	H8/H6	H1′	H2′/H2″	H3′	H4′	H5′/H5″	H2/Me	NH
A^{8Me}		6.09	2.42–2.54	4.89	4.21	3.58–3.73	7.65–2.28	
G	8.13	6.02	2.81–3.03	5.04	4.47	4.14		11.57
G	7.74	5.95	2.64	4.98	4.50	4.32		11.36
G	7.67	6.25	2.51–2.66	4.88	4.49	4.26		11.05
T	7.35	6.08	2.17	4.47	4.06	4.22	1.61	
T	7.20	5.88	1.75–2.22	4.60	3.94	3.48	1.65	
A^{8Me}		6.03	2.55	4.90	4.51	3.93	7.78–2.45	
G	8.05	6.01	2.49–2.77	5.03	4.45	4.17		11.56
G	7.72	5.95	2.64	4.99	4.46	4.28		11.27
G	7.67	6.24	2.52–2.67	4.90	4.49	4.26		10.97
T	7.35	6.07	2.16	4.46	4.04	4.20	1.60	

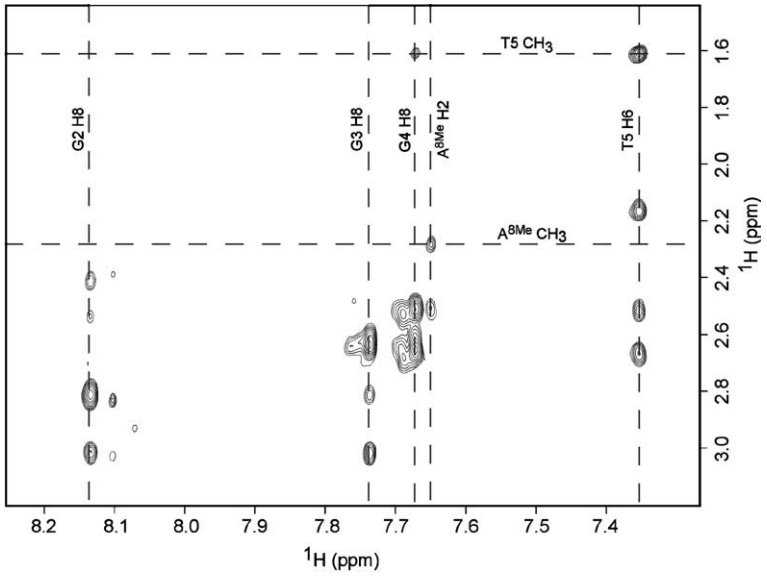

Figure 2. Expanded region of a NOESY spectrum (500 MHz, 180 ms mixing time, T = 30 °C) containing aromatic and H2′/H2″ sequential crosspeaks and NOEs involving methyl groups of **I**.

calculation for both quadruplex structures. Furthermore, in accordance to the observed ^{31}P chemical shifts,[21–23] backbone torsion angles were restricted to be in a range of ±20° of helical values of the natural quadruplexes [d(AGGGT)]$_4$ and [d(TAGGGT)]$_4$.[6] According to NMR data, glycosidic torsion angles for all guanines and thymines were fixed in the *anti*-domain (−157°/−117°), while a range of 0°/90° (*syn*-conformation) was used for χ angles of A^{8Me} residues.

The structure calculations on the two molecules **I** and **II** were undertaken by using restrained distance geometry calculations (CYANA).[27] The 10 out of 100 structures with the lowest CYANA target functions resulting from van der Waals and restraints violations were analysed in both cases and subjected to restrained energy minimization by using the force field CVFF (see experimental section). Particularly, average RMSD values of 1.30 ± 0.43 and 1.35 ± 0.37 for the backbone and all heavy atoms, respectively, were obtained from the superimposition of the 10 minimized structures obtained for **I**, while RMSD values of 1.96 ± 0.50 and 2.14 ± 0.46 were calculated for **II**, showing that the NOE restraints are largely satisfied for both complexes.

As expected, each strand of the complex formed by **I** possesses a right-handed helical backbone geometry and the same guanines from each of the four strands align in a plane to form three G-tetrads. As for A^{8Me} arrangement, they assume a almost planar arrangement and adopt a *syn*-conformation around the glycosidic bonds. Interestingly, while in the unmodified [d(AGGGT)]$_4$[6] two different patterns of H-bonds could be observed between H6 and N1 (named N61) and alternatively between H6 and N7 (named N67) (Fig. 3), the A^{8Me} residues seem to be characterized by neither pattern N61 nor N67, even though the mean structure suggests the formation of the N61 pattern of H-bond (Fig. 4).

In order to better understand the different behaviour of the 5′ end of **I** in comparison to the one of the unmod-

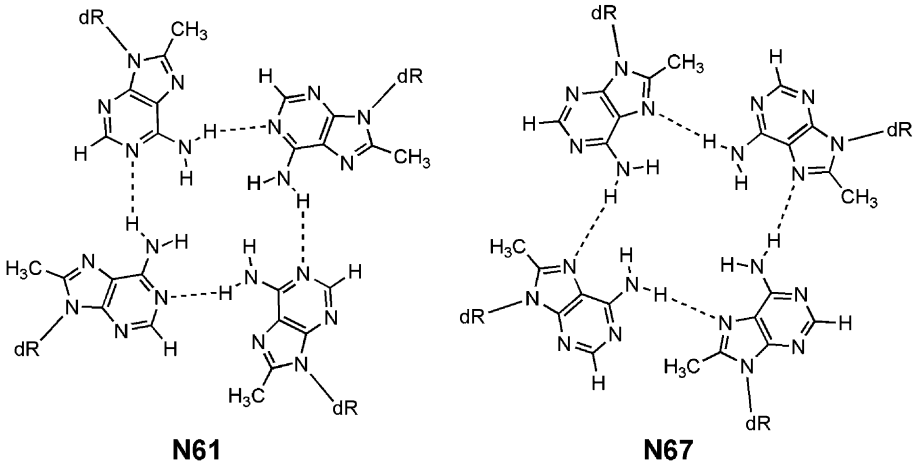

Figure 3. N61 and N67 H-bond patterns for an A-tetrad. H-bonds are indicated by dashed lines.

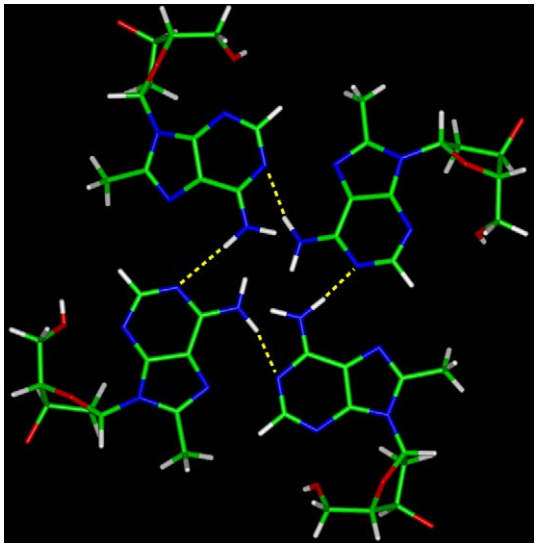

Figure 4. A^{8Me}-tetrad observed in the mean structure of **I**. Heavy atoms are depicted in colored 'stick' (carbons, green; nitrogens, blue; oxygens, red; hydrogens, white). Dashed yellow lines represent hydrogen bonds.

ified quadruplex, we performed further molecular modelling studies on **I**. Particularly, we have generated two models taking into account all the experimental constraints (interproton distances) and several structural features deduced from NMR studies, such as (i) the 4-fold symmetry and (ii) right-handed helicity of the overall structures, (iii) the *anti*-glycosidic conformation of all G and T residues, (iv) the *syn*-glycosidic torsion angle adopted by A^{8Me} nucleosides, (v) the presence of three G-quartets in a planar hydrogen bonded arrangement. The two models only differ for the H-bonds pattern, namely N61 and N67. The models clearly showed that the formation of both N61 and N67 patterns of H-bond are equally possible, thus suggesting that the slight line broadening suffered by the signals belonging to A^{8Me} residues and the consequent lack of a sufficient number of constraints at the 5′-end of the molecule might have prevented the right definition of that part of the molecule.

As for the structures obtained for **II**, they are characterized by a remarkable conformational disorder at 5′-TA^{8Me}-3′ step. Even if the resulting mean structure shows the possibility of formation of an A^{8Me}-tetrad with all residues in *syn*-conformation and held together by H-bond between A^{8Me}-amino hydrogen of one base and nitrogen N6 of the adjacent one, the A^{8Me} residues in the single structures deviate a lot from planarity and the stacking with the adjacent G-quartet is rather poor. By contrast, the 5′-GGGT-3′ tracks of the molecule resemble perfectly the structures of $[d(A^{8Me}GGGT)]_4$ and of their natural counterparts.[6] Molecular modelling studies were performed in order to better understand this disorder. As in **I**, two models were built taking into account all structural features deduced from NMR studies and imposing in the calculations either the H-bond pattern N61 or N67. The two models generated for **II** reveals that methyl groups of A^{8Me} residues seem to suffer of steric effects due to their interaction with deoxyribose rings of the previous residue (T) of each strand. Particularly, this is mainly evident when the formation of H-bond pattern N61 is forced (Fig. 5), whereas the presence of the methyl groups of A^{8Me} makes the formation of the hydrogen bonds of the type N67 possible only on condition that the planarity for the four modified adenines is lost. These results may suggest a possible explanation for the absence of a good definition of the 5′-edge of the complex, indicating that the terminal thymine bases at 5′-edge exert a very relevant influence on the arrangement of the underneath residues.

In order to estimate the effects of the substitution of a regular A residue with an A^{8Me} one on the thermal stability of the resulting quadruplex structures were further analysed by CD thermal denaturation experiments. The melting profile of **I**, **II** and their natural counterparts recorded at 264 nm give well-shaped sigmoid curves (Fig. 6). The T_m values, calculated as the maximum of the first derivative plots of molar ellipticity versus temperature, are listed in Table 2. These data show that thermal stability of both **I** and **II** are quite similar to that observed for the reference structures, thus suggesting that the incorporation of a methyl group does not affect the

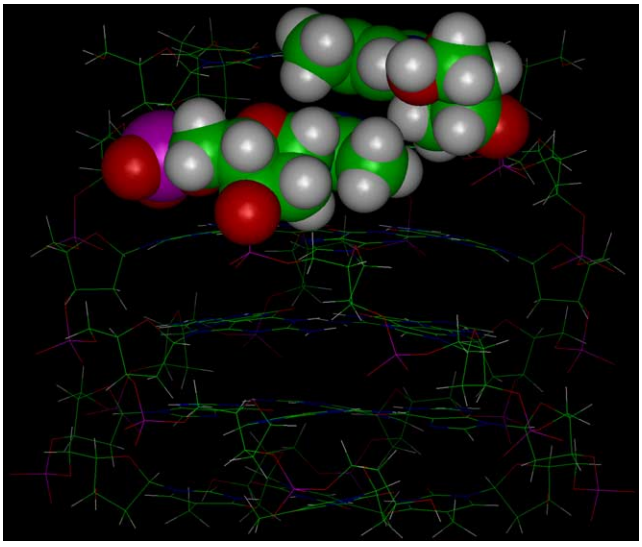

Figure 5. Side view of average structure of the best 10 structures of **II**. Heavy atoms are shown with different colors (carbons, green; nitrogens, blue; oxygens, red; hydrogens, white). One A^{8Me} residue and the dT residue of the same strand are reported in CPK. Steric effect between methyl of A^{8Me} and the dT residue is plainly observable.

quadruplex stability. Data acquired for **I** and **II** differ from the ones obtained by some of us for ODNs with the same sequences and containing 8-propynyl-2′-deoxyadenosine (A^{Pr}-ODNs),[28,29] whose thermal stability resulted to be higher than the natural counterparts. In order to find a possible explanation of the different behaviour of the A modified containing ODNs, detailed thermodynamic analyses of A^{Pr}-ODNs have been carried out and will be published elsewhere,[30] while similar analyses of A^{Me}-ODNs are currently in progress.

3. Conclusions

In this paper we report the synthesis and a structural study by NMR and molecular mechanics and dynamics calculation of the ODNs A^{8Me}-GGGT (**I**) and TA^{8Me}-GGGT (**II**), where A^{8Me} represents 8-methyl-2′-deoxyadenosine. Our results indicate that both oligonucleotides **I** and **II** form a parallel four stranded quadruplex in solution. As expected, NOE patterns involving 8-methyl group in A^{8Me} residues allowed us to define the main structural features of the 5′-end of the complexes. Particularly inter- and intra-strand NOEs show a *syn*-orientation and a symmetrical arrangement of A^{8Me} bases stacking on the adjacent G-tetrad for both quadruplex structures. Unfortunately, we were not able to detect signals attributable to hydrogen bonded 6-NH_2 group of A^{8Me} residues as Patel et al.[6] have observed just in the case of the natural counterpart of **I**. However, Searle et al.[8] in a study concerning the parallel quadruplex $[d(TGGAGGC)]_4$, suggest that the presence of a strong hydrogen bond might not be a feature of A-tetrad stabilization. Regarding oligonucleotide **II,** we also found a *syn*-orientation for A^{8Me} bases, in contrast with the above cited report[6] where the natural counterpart of **II** adopts an *anti*-glycosidic conformation. These data suggest that A^{8Me} can be regarded as a convenient and useful probe for glycosidic conformational preferences. On the other hand the molecular modelling studies suggest probable steric effects due to the methyl group that perturb the planarity of the modified adenines.

Table 2. Melting temperature of **I**, **II** and their natural counterparts

	T_m (°C)
$[d(AGGGT)]_4$	63
$[d(A^{8Me}GGGT)]_4$ (**I**)	61
$[d(TAGGGT)]_4$	67
$[d(TA^{8Me}GGGT)]_4$ (**II**)	68

Thermal stabilities of both **I** and **II** are relatively similar to those detected for their unmodified counterparts suggesting that the presence of A^{8Me} bases does not significantly affect the quadruplex stability.

The incorporation of A^{8Me} into a DNA synthetic sequence might be of interest at the level of ON-based therapeutics, a research area which yielded, so far, various type of pharmacologically active molecules.[31] Among these, aptamers are of particular importance since they can be generated against a wide variety of biologically significant targets (both proteins and small molecules) through iterative in vitro selection techniques (SELEX).[13] The scaffold of several aptamers is based on G-quadruplex structures and the presence of modified bases could, in principle, improve the biological activity. In this frame, A^{8Me} appears to be a useful vehicle to introduce an alkyl group into the aptamer grooves, potentially able to establish hydrophobic contacts with the target molecule, thus improving the interaction.

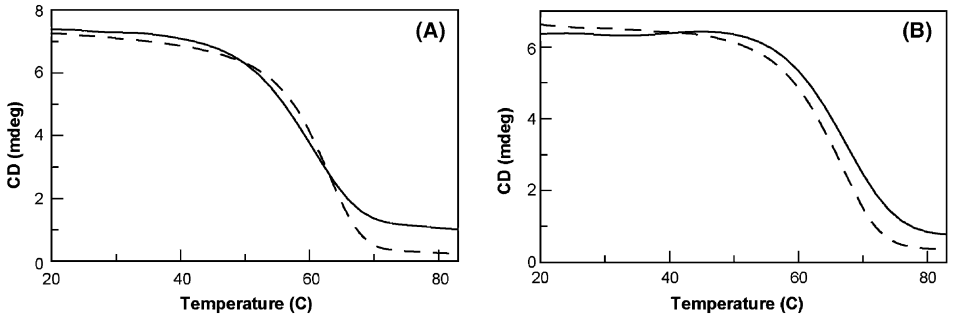

Figure 6. CD thermal denaturation profile of $[d(A^{8Me}GGGT)]_4$ (**I**) (——) and $[d(AGGGT)]_4$ (---) (A); $[d(TA^{8Me}\ GGGT)]_4$ (**II**) (——) and $[d(TAGGGT)]_4$ (---) (B).

The behaviour of A^{8Me} residues in sequences potentially able to form A-tetrads in other parallel and/or antiparallel quadruplex structures is currently in progress in our laboratory.

4. Material and methods

4.1. Synthesis of the oligonucleotides

Oligonucleotides **I**, **II** and their natural counterparts were synthesized on a Millipore Cyclon Plus DNA synthesizer, using solid phase β-cyanoethyl phosphoramidite chemistry at 15 μmol scale. The oligomers were detached from the support and deprotected by treatment with concd aqueous ammonia at 55 °C for 12 h. The combined filtrates and washings were concentrated under reduced pressure, redissolved in H_2O and analysed and purified by HPLC on a Nucleogel SAX column (1000-8/46, Macherey-Nagel, Düren, Germany); using buffer A: 20 mM KH_2PO_4 aq solution, pH 7.0, containing 20% (v/v) CH_3CN; buffer B: 1 M KCl, 20 mM KH_2PO_4 aq solution, pH 7.0, containing 20% (v/v) CH_3CN; a linear gradient from 0% to 100% B in 30 min. and flow rate 1 mL/min. were used.

All oligomers resulted to be more than 98% pure (NMR).

4.2. Nuclear magnetic resonance

The NMR samples had a concentration of approx 5 mM, in 0.6 mL (H_2O/D_2O 9:1) buffer solution having 10 mM KH_2PO_4, 70 mM KCl, 0.2 mM EDTA, pH 7.0. For D_2O experiments, the H_2O was replaced by drying down the sample, lyophilization and redissolution in D_2O. NMR spectra were recorded with a Varian UnityINOVA 500 MHz spectrometer at 30 °C. ^1H chemical shifts were referenced relative to external sodium 2,2-dimethyl-2-silapentane-5-sulfonate (DSS), whereas ^{31}P chemical shifts were referenced to external phosphoric acid (H_3PO_4 85% v/v). 1D proton spectra of samples in H_2O were recorded using the watergate sequence.[18] Phase sensitive NOESY spectra[32] were recorded with mixing times of 100 and 180 ms (T = 30 °C). The watergate technique was also used for acquiring NOESY spectra in H_2O. TOCSY[33] spectra with mixing times of 120 ms were recorded with D_2O solution. NOESY and TOCSY were recorded using the TPPI[34] procedure for quadrature detection. In all 2D experiments the time domain data consisted of 2048 complex points in t_2 and 400-512 FIDs in t_1 dimension. The relaxation delay was kept at 1.2 s for all experiments. The NMR data were processed on a SGI Octane workstation using FELIX 98 software (Accelrys, San Diego, USA).

4.3. Structure calculations

The structure calculations were performed with the program CYANA[27] starting from 200 random conformations. Upper limit distance constraints for both exchangeable and nonexchangeable hydrogens were classified according to the intensity of the cross peaks in the NOESY spectra (with 180 ms mixing time) with the CALIBA tool of the program CYANA.[27] Pseudoatoms were introduced where needed. 336 distance constraints for **I** and 320 for **II** were derived from NOE peak intensities and reduced to 206 and 160, respectively, after removal of the irrelevant ones. Hydrogen bonds constraints (16 upper and 16 lower limit constraints/G-tetrad: HN1–O6, N1–O6, HN2–N7, N2–N7) were incorporated with upper and lower distance limits of 2.0 Å and 1.7 Å for the hydrogen-acceptor distance and 3.0 Å and 2.7 Å for the donor–acceptor distance, respectively. These constraints for H-bonds did not lead to an increase in residual constraints violation. In accordance to the observed ^{31}P chemical shifts,[21–23] backbone torsion angle constraints were restricted to be in a range of ±20° with the respect of the angles of the unmodified quadruplexes. Glycosidic torsion angles for all guanines were kept in a range of −190°/−140° (*anti*-conformation), whereas a range of −157°/−117° (*anti*-conformation) was used for thymine residues. The 10 structures with the lowest CYANA target functions were subjected to energy minimization (with no angle constraints) using the conjugate gradient method and the CVFF force field as implemented in the program DISCOVER (Accelrys, San Diego, USA). During energy minimization, interproton distances and H-bond constraints involving G-tetrads were used with a force constant of 20 and 100 kcal mol^{-1} Å-2, respectively. Illustrations of structures were generated with the INSIGHT II program (Accelrys, San Diego, USA). All the calculations have been performed on a SGI Octane workstation.

4.4. Circular dichroism and CD melting experiments

CD samples of **I**, **II** and their natural counterparts $[d(AGGGT)]_4$ and $[d(TAGGGT)]_4$ were prepared at a concentration of 2.5×10^{-5} M, by using the buffer solution used for NMR experiments: 10 mM KH_2PO_4, 70 mM KCl, 0.2 mM EDTA, pH 7.0. CD spectra of all quadruplexes and CD melting curves were registered on a Jasco 715 circular dichroism spectrophotometer in a 0.1 cm pathlength cuvette. For the CD spectra, the wavelength was varied from 220 to 340 nm at 5 nm min^{-1} and the spectra recorded with a response of 16 s, at 2.0 nm bandwidth and normalized by subtraction of the background scan with buffer. The temperature was kept constant at 20 °C with a thermoelectrically controlled cell holder (Jasco PTC-348).

CD melting curves were registered as a function of temperature from 20 to 90 °C at 264 nm for all quadruplexes. The CD data were recorded in the same buffer as used for NMR experiments in a 0.1 cm pathlength cuvette with a scan rate of 1 °C m^{-1}.

Acknowledgements

This work is supported by Italian M.U.R.S.T. (P.R.I.N. 2002 and 2003) and Regione Campania (L.41, L.5). The authors are grateful to 'Centro Ricerche

Interdipartimentale di Analisi Strumentale', C.R.I.A.S., for supplying NMR facilities.

References and notes

1. Smirnov, I.; Shafer, R. H. *Biopolymers* **2001**, *56*, 209–227.
2. Simonsson, T. *Biol. Chem.* **2001**, *382*, 621–628.
3. Arthanari, H.; Bolton, P. H. *Chem. Biol.* **2001**, *8*, 221–230.
4. For a general recent review see: Davis, J. T. *Angew. Chem., Int. Ed.* **2004**, *43*, 668–698.
5. Esposito, V.; Randazzo, A.; Piccialli, G.; Petraccone, L.; Giancola, C.; Mayol, L. *Org. Biomol. Chem.* **2004**, *2*, 313–318.
6. Patel, P. K.; Koti, A. S. R.; Hosur, R. V. *Nucleic Acids Res.* **1999**, *27*, 3836–3843.
7. Gavathiotis, E.; Searle, M. S. *Org. Biomol. Chem.* **2003**, *1*, 1650–1656.
8. Searle, M. S.; Williams, H. E. L.; Gallagher, C. T.; Grant, R. J.; Stevens, M. F. G. *Org. Biomol. Chem.* **2004**, *2*, 810–812.
9. Patel, P. K.; Hosur, R. V. *Nucleic Acids Res.* **1999**, *27*, 2457–2464.
10. Patel, P. K.; Bhavesh, N. S.; Hosur, R. V. *Biochem. Biophys. Res. Commun.* **2000**, *270*, 967–971.
11. Meyer, M.; Schneider, C.; Brandl, M.; Suehnel, J. *J. Phys. Chem. A* **2001**, *105*, 11560–11573, and references cited therein.
12. Chen, J.; Zhang, L. R.; Min, J. M.; Zhang, L. H. *Nucleic Acids Res.* **2002**, *30*, 3005–3014.
13. For a recent review see: Rimmele, M. *Chem. Bio. Chem.* **2003**, *4*, 963–971.
14. Eason, R. G.; Burkhardt, D. M.; Phillips, S. J.; Smith, D. P.; David, S. S. *Nucleic Acids Res.* **1996**, *24*, 890–897.
15. Van Aerschot, A. A.; Mamos, P.; Weyns, N. J.; Ikeda, S.; De Clercq, E.; Herdewijn, P. A. *J. Med. Chem.* **1993**, *36*, 2938–2942.
16. Gait, M. J. In *Oligonucleotide Synthesis*; IRL: Oxford, 1984; pp 25–27.
17. Gait, M. J. In *Oligonucleotide Synthesis*; IRL: Oxford, 1984; pp 27–28.
18. Gait, M. J. In *Oligonucleotide Synthesis*; IRL: Oxford, 1984; pp 41–45.
19. Sklenar, V.; Piotto, M.; Leppik, R.; Saudek, V. *J. Magn. Reson.* **1993**, *102*, 241–245.
20. Wang, K. Y.; Mc Curdy, S.; Shea, R. G.; Swaminathan, S.; Bolton, P. H. *Biochemistry* **1993**, *32*, 1899–1904.
21. Wijmenga, S. S.; van Buuren, B. N. M. *Prog. Nucl. Mag. Reson. Spectrosc.* **1998**, *32*, 287–387.
22. Gorenstein, D. G. In *Phosphorus-31 NMR: Principles and Applications*; Gorenstein, D. G., Ed.; Academic: New-York, 1984.
23. Roongta, V. A.; Jones, C. R.; Gorenstein, D. G. *Biochemistry* **1990**, *29*, 5245–5258.
24. Jin, R.; Gaffney, B. L.; Wang, C.; Jones, R. A.; Breslauer, K. J. *Proc. Natl. Acad. Sci. U.S.A.* **1992**, *89*, 8832–8836.
25. Wüthrich, K. *NMR of Proteins and Nucleic Acids*; Wiley: New York, 1986.
26. Smith, F. W.; Feigon, J. *Biochemistry* **1993**, *32*, 8683–8692.
27. Guntert, P.; Mumenthaler, C.; Wuthrich, K. J. *Mol. Biol.* **1997**, *273*, 283–298.
28. Catalanotti, B.; Galeone, A.; Gomez-Paloma, L.; Mayol, L.; Pepe, A. *Bioorg. Med. Chem. Lett.* **2000**, *10*, 2005–2009.
29. Esposito, V.; Randazzo, A.; Galeone, A.; Varra, M.; Mayol, L. *Bioorg. Med. Chem.* **2004**, *12*, 1191–1197.
30. Petraccone, L.; Erra, V.; Esposito, V.; Randazzo, A.; Galeone, A.; Barone, G.; Giancola, C. *Biopolymers*, in press.
31. Opalinska, J. B.; Gewirtz, A. M. *Nat. Rev. Drug Discov.* **2002**, *1*, 503.
32. Jeener, J.; Meier, B. H.; Bachmann, P.; Ernst, R. R. *J. Chem. Phys.* **1979**, *71*, 4546–4553.
33. Braunschweiler, L.; Ernst, R. R. *J. Magn. Reson.* **1983**, *53*, 521–528.
34. Marion, D.; Wuthrich, K. *Biochem. Biophys. Res. Commun.* **1983**, *113*, 874–967.